Quantitative explanation for the electrical conductivity in $(La_{1-x}Y_x)_{2/3}Ca_{1/3}MnO_3$

2000 J. Phys.: Condens. Matter 12 L337

(http://iopscience.iop.org/0953-8984/12/22/102)

J. Phys.: Condens. Matter **12** (2000) L337–L344. Printed in the UK PII: S0953-8984(00)12955-8

LETTER TO THE EDITOR

Quantitative explanation for the electrical conductivity in $(La_{1-x}Y_x)_{2/3}Ca_{1/3}MnO_3$

S L Yuan†, J Q Li‡, G Li†, Y Jiang†, X Y Zeng†, Y P Yang‡ and S Z Jin§

† Department of Physics, Huazhong University of Science and Technology, Wuhan 430074, People's Republic of China

‡ Department of Physics, Wuhan Automotive Polytechnic University, Wuhan 430070, People's Republic of China

§ Structure Analysis Centre, University of Science and Technology of China, Hefei 230026, People's Republic of China

Received 28 March 2000

Abstract. The electrical conductivity of single-phase $(La_{1-x}Y_x)_{2/3}Ca_{1/3}MnO_3$ ceramic samples shows activated insulating behaviour at high temperatures, and a transition to metallic behaviour at low temperatures. On the basis of paramagnetic resonance experiments, we model the conductive channel as a series of paramagnetic regions and ferromagnetic domains along the direction of current flow. It is shown that the electrical conductivity can be explained quantitatively for the whole temperature range studied.

The discovery of colossal magnetoresistance (CMR) in the mixed manganese oxides $Re_{1-x}B_xMnO_3$ (Re = rare-earth cation, B = alkaline-earth cation) has aroused renewed interest in these systems [1]. It is commonly found that the CMR has a temperature-dependent behaviour similar to that for the zero-field resistance against T, and the largest CMR effect appears at the insulator–metal (I–M) transition. Clearly, in order to reveal the true nature of the CMR effect, one needs to understand the origin of the I–M transition. The traditional understanding is generally based on the double-exchange (DE) mechanism [2]. However, theoretical considerations [3] indicate that the DE mechanism alone could not quantitatively account for the observed transport properties, and other effects should be included. Electron–phonon coupling [4], small polarons [5], magnetic polarons [6], and spin polarons [7] have been commonly invoked in discussing the conductive behaviour in the manganese perovskites. Some purely empirical expressions for the T-dependent resistance have also been proposed [8,9] that take into account two parallel conductive channels: activated semiconductor-like behaviour at high temperatures and metallic behaviour at low temperatures. These mechanisms or models can explain the I–M transition, but do not provide a satisfactory fit to the experimental data over a wide temperature range. To study the conductive features in more detail, here we present new zero-field R-versus-T data on single-phase ceramic samples of $(La_{1-x}Y_x)_{2/3}Ca_{1/3}MnO_3$. On the basis of electron paramagnetic resonance (EPR) experiments, we assume the conductive channel to be a series of magnetic junctions, each consisting of a paramagnetic (PM) region sandwiched between adjacent ferromagnetic (FM) domains, and show that the experimental findings can be quantitatively explained over the whole temperature range studied.

A series of ceramic samples with nominal composition $(La_{1-x}Y_x)_{2/3}Ca_{1/3}MnO_3$ were prepared by the standard solid-state reaction. The phase purity for each sample was checked by x-ray diffraction and no spurious phase was found. Resistance (R) as a function of temperature

0953-8984/00/220337+08$30.00

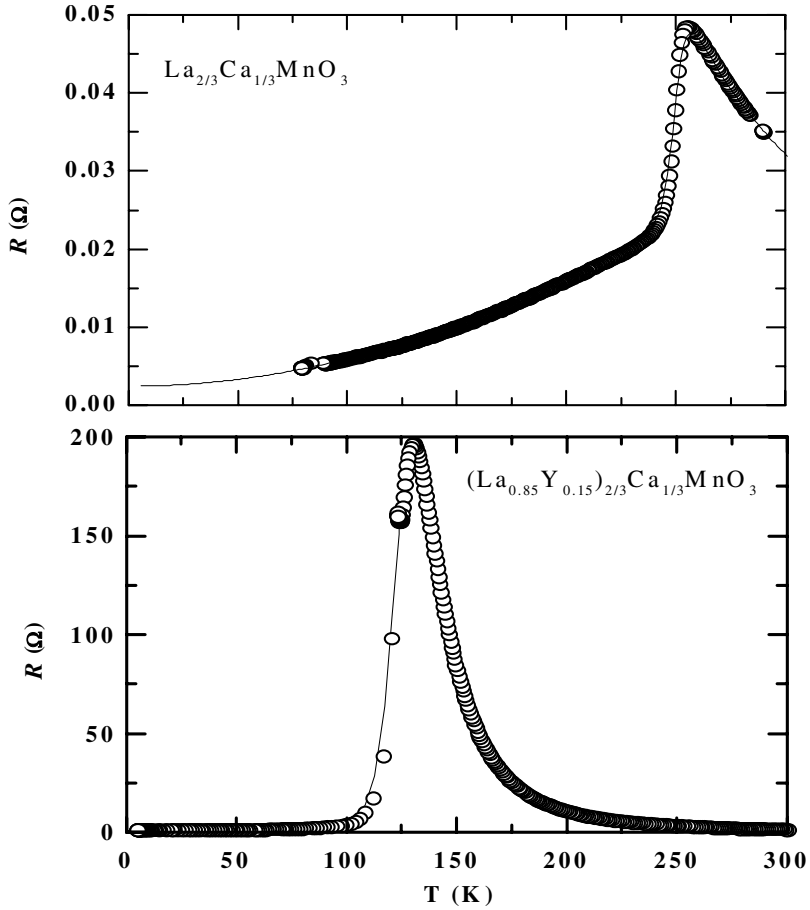

Figure 1. Zero-field R-versus-T curves for $(La_{1-x}Y_x)_{2/3}Ca_{1/3}MnO_3$ ($x = 0$, 0.1, 0.15, and 0.2). The solid lines are fits to equation (2), as discussed in the text.

was measured by the standard four-probe method on cooling. Figure 1 shows the R-versus-T dependence measured in zero magnetic field for samples with $x = 0$, 0.1, 0.15, and 0.2. Replacing La with smaller Y decreases the average A-site ionic size, $\langle r_A \rangle$, which strongly affects the transport properties. The main experimental features are summarized here.

(1) Each of the samples studied exhibits an I–M transition at a temperature close to the Curie temperature T_c.
(2) At $T \gg T_c$, the electrical conductivity shows an activated insulating behaviour that follows well an e^{E_g/k_BT}-dependence, while at $T \ll T_c$ there is a metallic behaviour in which the resistance smoothly decreases on cooling and which can be well described by a T^2-dependence.
(3) Near T_c, the resistance deviates clearly from the e^{E_g/k_BT}-dependence on cooling towards T_c, reaches the maximum (R_{max}) at T_c, and then steeply decreases on further cooling.
(4) Decreasing $\langle r_A \rangle$ substantially decreases T_c and substantially increases R_{max}.

Although the DE mechanism is shown to be incompatible with many aspects of the experimental data, it is a good physical basis for the discussion of these fascinating properties.

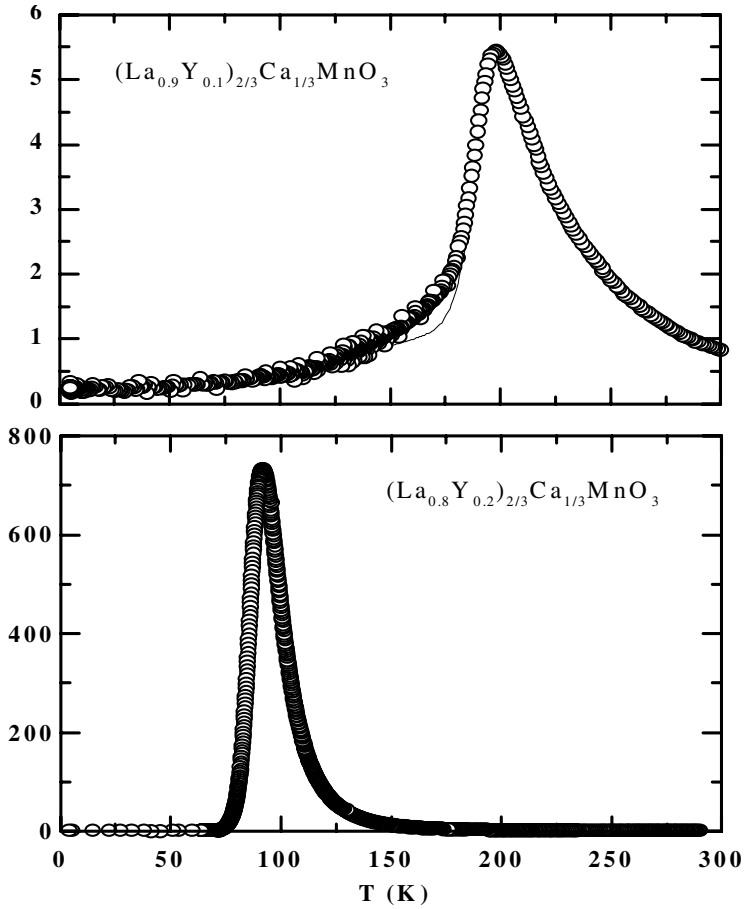

Figure 1. (Continued)

At $T > T_c$, the system is paramagnetic, and the conductivity shows activated insulating behaviour due to disorder scattering from charge carriers with different spin orientations. Below T_c, the DE interaction between Mn^{3+} and Mn^{4+} mediates FM coupling that favours the charge carriers transferring between adjacent Mn ions, leading to a transition to metallic behaviour. This implies that the I–M transition is of magnetic origin. The temperature T_c, determined by measuring the magnetization or magnetic susceptibility, is usually understood to be a temperature at which the PM–FM transition occurs. However, the question of the ground state at $T > T_c$ is subtle. Some experiments seem to give evidence for the existence of short-range magnetic correlation well above T_c—such as neutron scattering [10, 11] and small-angle neutron scattering [12] measurements. If this is present, it can be checked with the help of the EPR technique because of its sensitivity to magnetic heterogeneity.

EPR experiments were performed at 9.46 GHz using a Bruker (ER-200D-SRC) reflection X-band-type spectrometer at various constant temperatures by sweeping the magnetic field from 0 to 6000 Oe. The temperature for each measurement was controlled to an accuracy of ± 0.1 K using the Bruker N_2 temperature controller. All the samples show common features in their resonance behaviours. At high temperatures, the resonance spectrum consists of a single line with a Lorentzian lineshape. With decreasing temperature, the resonance field remains

constant, the derivative signal intensity greatly increases, and the peak-to-peak linewidth ΔH_{pp} becomes narrow. The symmetric signal with the Lorentzian lineshape is maintained to a temperature T_{onset}. Below this temperature, some distortions of the lineshape occur: the derivative signal intensity becomes weak, the resonance line broadens substantially, and the resonance field clearly shifts to a lower value. These observations suggest that the real PM region corresponds to a temperature range of $T > T_{onset}$, but in the temperature range of $T_c < T < T_{onset}$ the anomalous PM phenomena occur. Also, our experiments show that the onset temperature (T_{onset}) for the anomalous PM behaviour strongly depends on $\langle r_A \rangle$, varying from $\sim 1.15T_c$ for $x = 0$ to $\sim 2T_c$ for $x = 0.2$. Similar behaviour was also found in previous EPR experiments [13–17].

As seen in figure 1, $\langle r_A \rangle$ strongly affects the transition properties including the values of T_c and R_{max}. On the other hand, the relative onset temperature (T_{onset}/T_c) for the appearance of the PM anomaly increases with decreasing $\langle r_A \rangle$. This fact indicates some correlation between the PM anomaly and the I–M transition. Such a correlation becomes clearer if one plots both R and ΔH_{pp} as functions of temperature in the same figure. An example is presented in figure 2 for the $x = 0.15$ sample. It is found that ΔH_{pp} decreases almost linearly with decreasing T and reaches a minimum at T_{onset}. Its physical origin has been discussed in reference [16]: it is explained as being caused by both spin–lattice and exchange-narrowing spin–spin interactions. When temperature is decreased from T_{onset}, one finds that ΔH_{pp} increases anomalously with decreasing temperature. On the other hand, a substantial increase in R occurs in the temperature range of $T_c < T < T_{onset}$. It is interesting to find that in the anomalous PM regime, the transport shows a temperature-dependent behaviour similar to that for ΔH_{pp} against T. This finding provides an important clue to the understanding of the conduction behaviour.

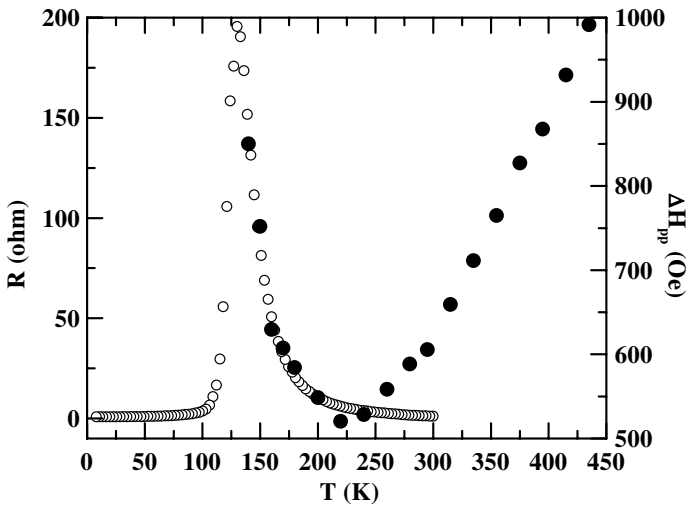

Figure 2. Temperature dependences of both R (open circles) and ΔH_{pp} (solid circles) obtained for $(La_{1-x}Y_x)_{2/3}Ca_{1/3}MnO_3$ ($x = 0.15$).

Manganese perovskites contain both Mn^{3+} and Mn^{4+} ions. Because of the double-exchange interaction, Mn^{3+} ions are ferromagnetically coupled to adjacent Mn^{4+} ions to form Zener pairs [2] (i.e., Mn^{3+}–Mn^{4+} pairs). At high temperatures, these Zener pairs are isolated and hence the system is still paramagnetic as a whole. Goodenough and Zhou [18] called it superparamagnetic ('PM' for short) to distinguish it from conventional paramagnetic systems. As is well known, the Mn-based oxides with perovskite-related structures can accomplish

a dynamic phase segregation because of cooperative atomic displacements. As a result of dynamic phase segregation, these Zener pairs become segregated into domains of short-range FM ordering within the 'PM' matrix. As long as no magnetic correlation exists between the domains, the system still exhibits 'PM' behaviour as a whole. On cooling, the FM domains grow, or equivalently, the separation distance between adjacent domains becomes shorter. On cooling below T_{onset}, the FM domains themselves are no longer isolated, and one needs to consider the magnetic correlation between them. Because of the magnetic correlation, the system below T_{onset} does not show 'PM' behaviour any longer. This leads to the occurrence of some distortions in the resonance behaviour. On further cooling below T_c, the FM domains tend to overlap, so the system enters a long-range FM regime. We should point out that the magnetic feature mentioned here is in agreement with previous experimental observations—for example, through small-angle neutron scattering [12] and scanning tunnelling spectroscopy [19] measurements.

We consider Zener pairs to be charge carriers that can move most easily when their spins point in the same direction. Clearly, the conductivity is metallic within the FM domain, but insulating in the 'PM' region due to disorder scattering from charge carriers with different spin orientations. As already discussed, the observed anomalous paramagnetic behaviour is due to the magnetic correlation between the FM domains. Because of the correlation, the system looks like a network of magnetic coupled junctions. Each junction consists of a 'PM' region sandwiched between two FM domains. The conduction of the junction depends on various factors, but most notably on the thickness of the 'PM' region and the relative orientation of the magnetic moment in the domains. As long as the 'PM' region is sandwiched between the domains, the system always exhibits thermally activated insulating conductivity behaviour, while when the domains overlap with each other (or equivalently, the thickness of the 'PM' region becomes zero), the system shows metallic conductivity. This implies that the I–M transition is due to the overlapping of FM domains.

To quantitatively take into account the feature mentioned above, we introduce a quantity, f, to represent the volume fraction of FM domains. The corresponding volume fraction of 'PM' regions is represented by $1 - f$. Clearly, $f = 0$ at $T \gg T_c$ and $f = 1$ at $T \ll T_c$, while

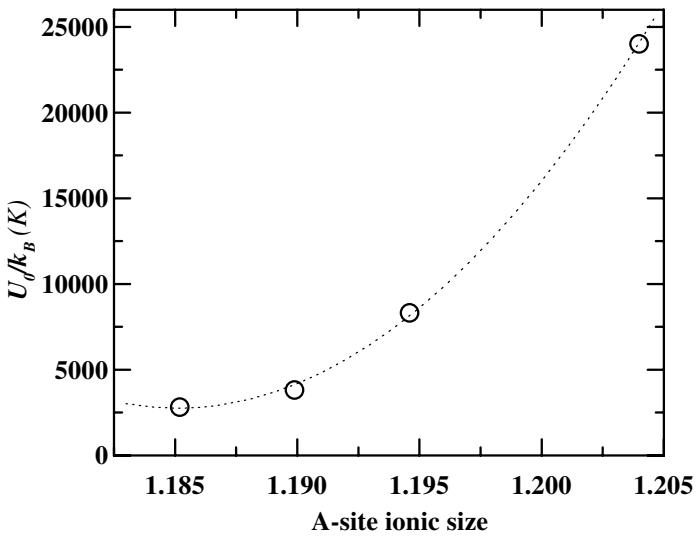

Figure 3. U_0 used in the calculation of equation (2) as a function of $\langle r_A \rangle$.

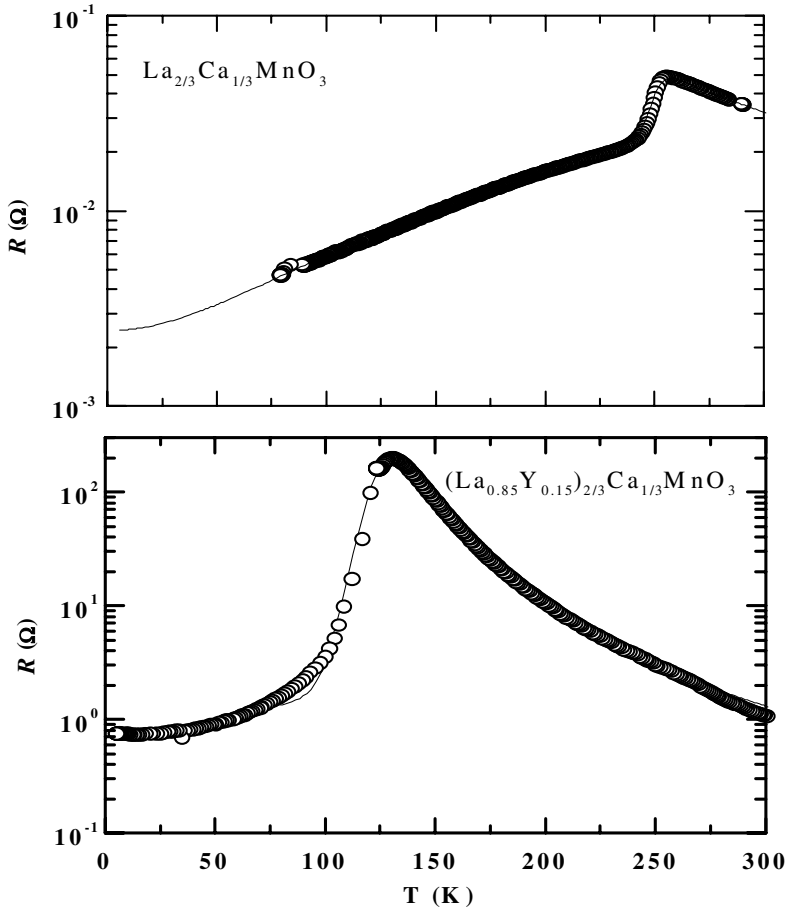

Figure 4. Replots of the zero-field R-versus-T curves shown in figure 1.

$0 < f < 1$ near T_c. An appropriate empirical expression for such a variation behaviour can be represented by

$$f = 1/(1 + e^{-U/k_B T}) \tag{1}$$

where $U = U_0(1 - T/T_c)$ and U_0 is a T-independent constant. Furthermore, we model the conductive channel as a series of 'PM' regions (the corresponding resistance is R_{PM} approximated by $R_{PM} = R_1 e^{E_g/k_B T}$) and FM domains (the corresponding resistance is R_{FM} approximated by $R_{FM} = bT^2$) along the direction of current flow. Regardless of the residual resistance, the total resistance (R) can be then represented as

$$R = (1 - f)R_{PM} + fR_{FM} = (1 - f)R_1 e^{E_g/k_B T} + fbT^2. \tag{2}$$

Equation (2) predicts well the PM insulating behaviour at $T \gg T_c$ for which $f = 0$ and $R = R_1 e^{E_g/k_B T}$, and the FM metallic behaviour at $T \ll T_c$ for which $f = 1$ and $R = bT^2$. Near T_c, $(1 - f)$ tends to become zero, while R_{PM} increases exponentially. They compete to yield a resistance maximum near T_c. To support our arguments, here we show that we can quantitatively fit equation (2) to the experimental data. Equation (2) is a fitting equation with one adjustable parameter, i.e., U_0, because the other parameters can be determined directly from experiments. Both R_1 and E_g can be easily obtained by plotting the high-T data in the

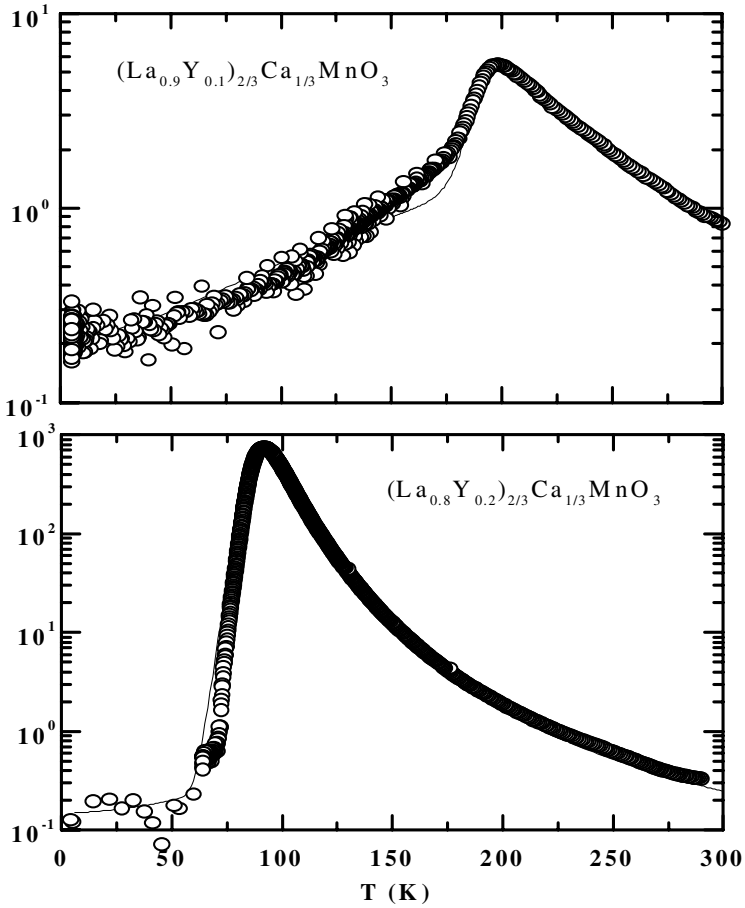

Figure 4. (Continued)

form of $\ln R$ versus $1/T$, b can be obtained by fitting to the low-T experimental data, and T_c corresponds to the I–M transition. These experimental parameters are listed in table 1. We then calculate the R-versus-T dependence on the basis of equation (2) using the fitting parameter U_0 shown in figure 3 for different samples. The calculated curves are shown in figure 1 together with the corresponding experimental curves. It can be seen that equation (2) yields excellent agreement with the experimental data for all the samples studied. To show the behaviour at low resistance levels, the calculated curves are re-displayed in figure 4 on

Table 1. Parameters extracted from the experimental data for $(La_{1-x}Y_x)_{2/3}Ca_{1/3}MnO_3$ ($x = 0$, 0.1, 0.15, and 0.2).

x	T_c (K)	R_1 (Ω)	E_g/k_B (K)	b (Ω K^{-2})
0	250	0.0025	766	3.5×10^{-7}
0.1	192	0.01657	1184	3.0×10^{-5}
0.15	127.3	0.02045	1250	1.0×10^{-4}
0.2	90.7	0.0058	1126	2.0×10^{-5}

semi-logarithmic plots together with the corresponding experimental curves. Clearly, even at low resistance levels the equation also gives excellent fits to the experimental observations. Small differences between the calculated and measured data at T slightly lower than T_c may be due to the assumption that $R_{\mathrm{FM}} \propto T^2$ being too simple.

In summary, we have experimentally studied the electrical conductive characteristics in zero field for $(La_{1-x}Y_x)_{2/3}Ca_{1/3}MnO_3$ ($x = 0$, 0.1, 0.15, and 0.2). EPR experiments reveal an important clue to the understanding of the electrical conductive characteristics. Modelling the system as a network of magnetic coupled junctions consisting of 'PM' regions sandwiched between adjacent FM domains, we demonstrate that the observed R-versus-T curves can be quantitatively explained over the whole temperature range studied. In the present approach, the correlation between magnetic and transport properties is considered by introducing a quantity f that represents the volume fraction of ferromagnetic domains.

This work was supported by the Trans-Century Training Programme Foundation for Talents by the Ministry of Education.

References

[1] Coey J M D, Viret M and von Molnar S 1999 *Adv. Phys.* **48** 167 and references therein
[2] Zener C 1951 *Phys. Rev.* **82** 403
[3] Millis A J, Littlewood P B and Shraiman B I 1995 *Phys. Rev. Lett.* **74** 5144
[4] Millis A J 1998 *Nature* **392** 147
[5] Mott N F 1993 *Conduction in Non-Crystalline Materials* (New York: Oxford University Press)
[6] Kusters R M *et al* 1989 *Physica* B **155** 362
[7] Zhang S 1996 *J. Appl. Phys.* **79** 4542
[8] Nunez-Regueiro J E and Kadin A M 1996 *Appl. Phys. Lett.* **68** 2747
[9] Sun J *et al* 1995 *Appl. Phys. Lett.* **67** 2726
[10] Lynn J W *et al* 1996 *Phys. Rev. Lett.* **76** 4046
[11] De Teresa J M *et al* 1996 *Phys. Rev.* B **54** 1187
[12] De Teresa J M *et al* 1997 *Nature* **386** 256
[13] Causa M T *et al* 1998 *Phys. Rev.* B **58** 3233
[14] Oseroff S B *et al* 1996 *Phys. Rev.* B **53** 6521
[15] Rettori C *et al* 1997 *Phys. Rev.* B **55** 3083
[16] Yuan S L *et al* 2000 *J. Phys.: Condens. Matter* **12** L109
[17] Yuan S L *et al* 2000 *J. Phys.: Condens. Matter* **12** L241
[18] Goodenough J B and Zhou J S 1997 *Nature* **386** 229
[19] Fath M *et al* 1999 *Science* **285** 540